Macromolecules
ARTICLE

Macromolecules **2010**, *43*, 7357–7367 **7357**
DOI: 10.1021/ma1011045

Free Volume Analysis and Transport Mechanisms of PVC Modified with Fluorothiophenol Compounds. A Molecular Simulation Study

Javier Sacristan* and Carmen Mijangos

Instituto de Ciencia y Tecnología de Polímeros (CSIC) C/Juan de la Cierva 3, 28008, Madrid, Spain

Received May 18, 2010; Revised Manuscript Received July 15, 2010

ABSTRACT: Molecular dynamics simulations using fully atomistic models were conducted to investigate gas transport mechanism and its connection to the free volume distribution and morphology in polyvinyl chloride (PVC) and in PVC modified with 4-fluorothiophenol. The influence of both, modification degree and temperature on diffusion mechanism was thoroughly studied. The diffusion coefficients of O_2 and N_2 were determined via molecular dynamics simulation using the COMPASS forcefield over a range of temperatures (375, 400, 425, and 450 K) using up to 200 ns simulation time. The introduction of pendant bulky groups along the polymer backbone results in a less ordered polymer matrix increasing the free volume available and consequently the diffusion coefficients of both gases, O_2 and N_2. Additionally, the temperature range selected in this work allows us to investigate the crossover from a solid-like diffusion mechanism (at low temperatures) to a liquid-like mechanism that takes place at higher temperatures. The gas transport coefficients of these polymers obtained from MD simulations were compared with previously reported values in literature based on both experimental and simulation studies, and the results obtained were within the expectations indicating the viability of the approach.

Introduction

Over the past few years, the study of gas diffusion in polymeric matrices based on their chemical structure holds extraordinary technological importance in the design of barrier and membrane materials.[1−3] One attractive approach in order to develop new polymeric membranes is modifying existing polymers, mainly due to its simplicity, reproducibility, and low cost. It is well-known that gas permeability of polymeric materials can be improved by restricting the motion of polymer chains.[4,5] This can be achieved in several ways such as, reducing the concentration of flexible linkages in the backbone,[6,7] attaching bulky side groups,[8−10] and cross-linking polymer chains.[11−13] Following these ideas, it is possible to prepare new materials with enhanced gas separation performance.

Nevertheless, the characterization and evaluation of transport properties of these materials are often very time-consuming. Molecular dynamics simulation has emerged as a powerful theoretical tool to successfully calculate diffusion coefficients of penetrant molecules in a variety of polymers[14,15] (and references therein). Moreover, it is a very valuable tool to understand the underlying diffusion mechanism and the relation between chemical structure and rate of diffusion giving information at a molecular level.[14,16−18] Previous studies showed that the mechanism of gas diffusion, at a molecular level, in polymers can be visualized as occurring by a hopping mechanism. The gas molecules oscillate most of the time inside microcavities in the polymer matrix. From time to time, due to cooperative motions of the polymer chain, a microtunnel appears joining two of these cavities which allow the gas molecules to jump into a neighboring cavity. The free volume is responsible for the existence of these cavities, and their distribution strongly depends on the polymer type and temperature.

In the literature, the transport of small penetrants in polymer systems has been studied by calculating the penetrant diffusivity from the mean square displacement (MSD) in either full MD simulations[19−26] or using the transition state approach, TST.[27−31] In both cases, a reasonable agreement with experimental values is reached. The diffusion coefficient of small gas molecules is calculated by means of the Smolouschski−Einstein equation $\langle |r(t) - r(0)|^2 \rangle = 6Dt$ but it only applies in the limit of large times at which the penetrant has performed enough jumps for its trajectory to become a random walk in the polymer model. Thus, for polymers with low diffusion coefficient values, longer simulation times and/or higher simulation temperatures are required to obtain reliable results. Several authors have shown that in materials with low diffusivities, ranging from amorphous to crystalline polymers, by using simulation times considerably longer than few nanoseconds and higher simulation temperatures, it is feasible to investigate the connection between experimental observation and detailed atomistic level events from computer simulations.[32−38]

In this study, the MD method is employed because unlike the transition state method, MD also provides information regarding the mechanisms of transport. As it was previously mentioned, transport properties of polymers are strongly dependent on many different factors such as, free volume and its distribution, density, temperature and pressure, crystallinity, polymer chain length, polymer mobility and packing, solute size, and affinity for the material. Therefore, our aim here is 2-fold; on the one hand, through molecular dynamic simulation on fully atomistic models understand the reasons underlying pure PVC relative low diffusivity in comparison with fluoride PVC, PVCF (PVC chemically modified with 4-fluorothiophenol; with a degree of modification in weight of 15% and 50%, PVC15F and PVC50F respectively). On the other hand, the second objective is to investigate the crossover from a solid-like diffusion mechanism (at low temperatures) to a liquid-like mechanism that takes place at higher temperatures giving at the same time a better insight in the diffusion mechanism of O_2 and N_2 through these materials as a function of temperature in the range 375−450 K. It is worthy of remark that PVC50F, PVC with a degree of substitution of 50%, has not yet

*Corresponding author. E-mail: jsacristan@ictp.csic.es.

Published on Web 07/29/2010

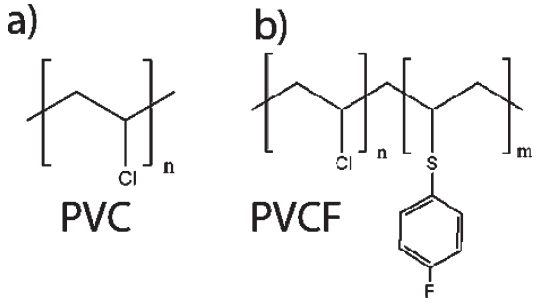

Figure 1. Two polymers under study, along with their acronyms. The number of monomers *n* is as follows: for PVC 150, for PVC15F 135, and for PVC50F 75, and the number of monomers modified by 4-fluorothiophenol *m* is 15 for PVC15F and 75 for PVC50F.

been synthesized. Therefore, this simulation also serves as a strategy for a systematic molecular design of new tailor-made membrane materials. We will also asses the importance of chain packing, free volume distributions and local chain mobility in relationship with gas transport properties in these materials. The estimation and analysis of these polymer properties will enhance our understanding of the differences in the values of the diffusion coefficients of a given penetrant in structurally different polymers.

Simulation Methodology

All simulations were performed using Material Studio 4.4 (MS4.4).[39] Two materials, pure Poly vinyl chloride (PVC) and fluorinated PVC in which chlorine atoms of the polymer chains were partially replaced by 4-fluorothiophenol, up to modification degrees of 15% (PVCF15) and 50% (PVCF50) were modeled using the fully atomistic force field, COMPASS.[40] This force field has been successfully used for a long time on the prediction of structural, conformational, and material properties for a broad number of polymers under a wide range of conditions of temperature and pressure.[41−43] These references also contain detailed comparisons to existing experimental data showing that the force field is realistic.

The repeat units of all investigated materials are shown in Figure 1. Generation and equilibration of amorphous cells was done according to the next procedure. First, 4-fluorothiophenol molecule was built through the Builder module of MS4.4 and subjected to energy minimization before polymerization. Next, single chains of the required length and composition were formed and packed utilizing the Polymerizer and Amorphous cell module of MS4.4. The simulation cells contain one polymer chain consisting of 150 repeat units. A single chain was used to minimize the chain ends effect on the simulation results. The statistical copolymer chains, PVC15F and PVC50F were formed using reactivity ratios of 0.85 for vinyl chloride and 0.15 for 4-fluorothiophenol and 0.5 for vinyl chloride and 0.5 for 4-fluorothiophenol, respectively. The amorphous cells of PVC15F and PVC50F were constructed at low densities, 0.6 gr cm^{-1} to minimize the time required for building the cells and to avoid ring catenations and spearing.[30,31,44] The cells were initially refined by the Basic_ Refine protocol of MS4.4.[39] Later each cell has to be further equilibrated to provide more realistic configurations. The initial velocities of the atoms were assigned using a Maxwell−Boltzmann distribution at the desired temperature and the Ewald summation method was used to calculate long-range electrostatic interactions with an accuracy value of 1.0×10^{-2} kcal mol^{-1}.[45] It is essential to be sure that the simulated systems are well equilibrated before the production runs, particularly at the lower simulated temperatures. In order to overcome this problem the constructed cells were subjected to equilibration consisting of various steps. Initially the energy of each generated cell was minimized to a convergence value of 0.01 (kcal/mol)/Å, using two different methods; first the steepest descends and then the conjugate gradient, relaxing the system to a local state of minimal potential energy. After minimization, the two conformations with the lowest energy were chosen. In order to prevent the system to be trap on a local high energy minimum, 0.5 ns of (constant number of particles, temperature and volume) *NVT*-MD simulation was performed at 600 K. The cells were cooled back to the target temperature using 25 K increments. *Next,* experimental density was reached by increasing the pressure with several cycles of (*constant particle number, pressure, and temperature*) *NPT*-MD and high temperature *NVT*-MD to further relax the polymer structure using the Berendsen thermostat and barostat using a half-life for decay to the target temperature of 0.1 and 0.1 ps for the pressure scaling constant.[46] The reason for this choice is that even using experimental densities as a starting point it is necessary to establish the equilibrium density which makes more unlikely that both fluctuations and the average value in the calculated pressure, lead to unacceptable inaccuracies in the calculation of any other property of the system. Each cell was pressurized to increase its density well above the experimental value, and then pressure was decreased in several stages to 1 bar. Once the models reach densities close enough to the experimental values, error ≤2%, 1 ns *NVT* dynamics were performed at 600 K, a temperature well above the glass transition temperature of the polymer, to ensure that the system is well-relaxed. Then the annealed cells were cooled back to the target temperature using 25 K increments. The duration of the NPT runs at each temperature was 250 ps.

The penetrant molecules, 8 oxygen and 8 nitrogen molecules, were randomly inserted at the free volume sites of the cells avoiding interatomic overlapping. After insertion of gas molecules the systems were further equilibrated through a series of 500 ps *NVT* and *NPT* runs at the target temperature and 1 bar of pressure in order to further improve the equilibration before using them for data production. The specific volume and energy was observed to fluctuate around a well-defined mean over the time scale of the dynamics, indicating that the equilibrium density and energy for the given temperature and pressure had been attained and the system is in the most probable configuration. Since the investigated copolymers are novel, neither the density nor other properties of interest in the present work, of these polymers has been previously reported in the literature. Thus, we have calculated them by applying the predictive capability of the Synthia program[47] in MS 4.4.[39] In Synthia, many polymer properties are expressed in terms of topological variables combined with geometrical variables and/or other structural descriptors used to obtain refined correlations. The remaining properties are calculated from relationships that express them in terms of the properties being calculated by using the topological variables. This method[48] enables the prediction of the properties of all polymers without being limited by the absence of the group contributions for the structural fragments from which a polymeric repeat unit is build. It is equivalent to the prediction of the properties by the summation of additive contributions mainly over atoms and bonds instead of groups. The accuracy and reliability of this methodology is as good as can be expected from any scheme based on simple quantitative structure-properties relationship. In this context it is worthy of remark the good agreement between the experimentally determined density values of pristine PVC, and modified PVC with fluorothiophenol groups, Table 1 (at 300 K) and the values predicted by Synthia program which clearly reflects the high accuracy and reliability of this methodology. The resulting densities of PVC, PVC15F and PVC50F cells, see Table 1, are close enough to experimental[5,49] and theoretical values, within the general reported range, ∼2%,[31,34,50] to expect only a small effect (of the density) on the diffusion results that may lead to an small overestimation of the diffusion coefficients due to the finite-size effect of the

Table 1. Experimental and Predicted Density and Cohesive Energy of PVC, PVC15F, and PVC50F at Different Temperatures[a]

	ρ^{exp}, gr cm^{-3}			ρ,[b] gr cm^{-3}					δ,[c] J cm^{-3}	δ^{Sim}, J cm^{-3}			
	300 K	373 K	393 K	300 K	375 K	400 K	425 K	450 K	300 K	375 K	400 K	425 K	450 K
PVC	1.387	1.352	1.334	1.382	1.328	1.301	1.277	1.258	19.5−22.1	18.4	17.6	17.3	16.9
PVC15F	1.355			1.335	1.305	1.282	1.264	1.243	19.1−21.5	15.9	15.7	15.2	14.5
PVC50F	1.306			1.305	1.28	1.257	1.241	1.201	18.2−20.5	15.7	15.5	13.7	12.9

[a] For comparison the corresponding experimental values obtained at 300, 373, and 393 K from refs 5 and 49 are also quoted. [b] Calculated with Synthia program[47] and used in MD simulations. [c] Calculated with Synthia program[47] following Fedors[54] and Van Krevelen[5] methods.

model, which do not affect any of the conclusions drawn from this work.

The equilibrated packing models were then subjected to *NPT*-MD data production runs at 375, 400, 425 and 450 K for a total of 150 ns at $T > 375$ K and 200 ns at 375 K. These relatively large simulation times are needed in order to ensure that normal diffusive regime is reached. It is worthy of remark that all simulations were carried out at $T > T_g$. After the first nanosecond MD run, seven more successive runs of 2, 10, 40, 80, 100, 150, and 200 ns were carried out, collecting data every 0.01, 0.05, 0,125, 0,250, 0.5, 1, and 1 ps, respectively.

The properties of interest in this work are diffusion coefficients obtained from the mean squared displacement (MSD) curves, fractional free volume (FFV) and its topology and distribution and intermolecular pair distribution functions (RDFs). As such, the most important criteria for equilibration are that these properties do not drift with time. We also require that at a minimum, the penetrant molecules have traveled, on average, a distance greater than the simulation box in order to ensure that true diffusion is observed within the simulation time window. The lack of drift following the equilibration period is illustrated in Figure 2a, where we plot the MSD of all polymer atoms of PVC and PVCF over five consecutive 20 ns blocks at 380 and 450 K (similar results, not shown here, were obtained at 400 and 425 K). No variations in block averages are observed over the duration of the successive runs confirming local equilibration of the sample. Moreover Figure 2b and Figure 3 display the intramolecular and intermolecular radial distribution function of the main chain carbons respectively which converge to zero and one confirming the local equilibration of the systems.[51]

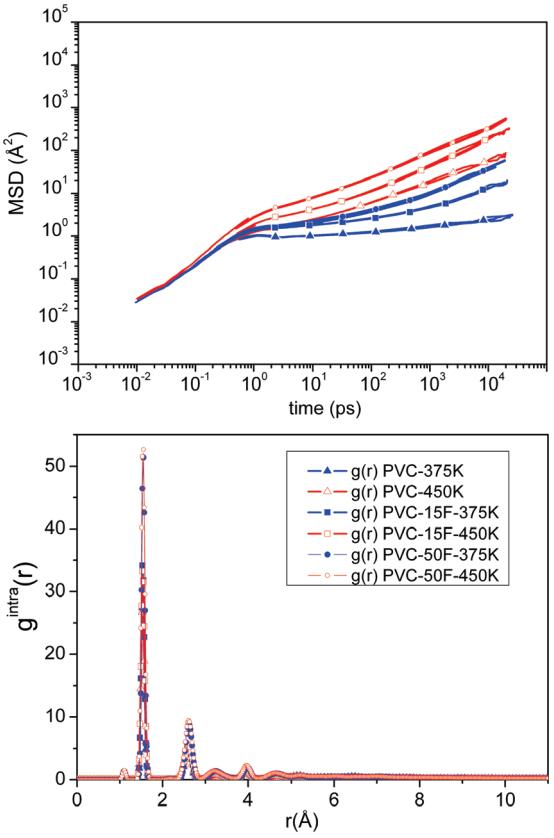

Figure 2. (a) Mean square displacement of all atoms in PVC (triangles), PVC15F (squares) and PVC50F (circles) calculated over four 20 ns blocks, different curves represent 20 ns consecutive blocks and (b) main chain carbon−carbon intramolecular radial distribution function.

Results and Discussion

Structural Features of the Packing and Cohesive Energy. Gas permeation performance of polymers is strongly related to their chemical composition and structural properties (density, free volume, chain packing, etc.).[14,52] These structural properties depend directly on the chemical nature of the constituent monomers.[19,53] However before obtaining reliable property predictions, one primal concern is to generate representative structures of the polymer matrix. The cohesive energy density (CED) is a key thermodynamic property of any polymer system representing the sum of all intermolecular interactions and it has been widely used to demonstrate the ability of the model to describe the real material. The cohesion of a polymer material originates from the intermolecular attractions, including van der Waals, hydrogen bonding, and Coulombic interactions. Normalization of the E_{coh} to molar volume (V) yields the cohesive energy density (CED). The solubility parameter, δ, is simply the square root of the CED and is a parameter of great importance in the field of thermodynamics of polymer blends. The CED and δ calculated directly from the simulation and δ is displayed in Table 1 together with experimental and calculated values from additive group contribution[5] by means of Synthia module[47] of Material Studio 4.4.[39] Before comparing the CED values it should be noted that theoretical values were calculated by means of two slightly different methods, Synthia−Fedors[54] and Synthia−van Krevelen[5] at 300 K meanwhile CED computed from MD runs was done at higher temperatures (T used in the production runs, 375, 400, 425, and 450 K). Small differences observed between these two methods are most likely due to the way that the group volumes are calculated. Therefore, due to these two factors some small differences should be expected between both sets of values but from a qualitative point of view it does not affect any of the conclusions that can be drawn from its analysis.

From Table 1, CED calculated values lie well within the empirical range of 14−28 (J cm^{-3})$^{1/2}$, reported for polymers[5] and are in good agreement with experimental results giving additional support to the model considered in this work. The higher solubility parameter of pristine PVC compared to fluoride PVC arises from the most favorable interactions among the PVC polar groups. Consequently the higher solubility parameter and the relatively smaller side group of pristine PVC compared to fluoride PVC should have an impact in the free volume available which should manifest in different diffusion coefficients and solubilities.[8,10,26]

Transport of small molecules through a polymer film is very sensitive to changes in polymer packing efficiency and

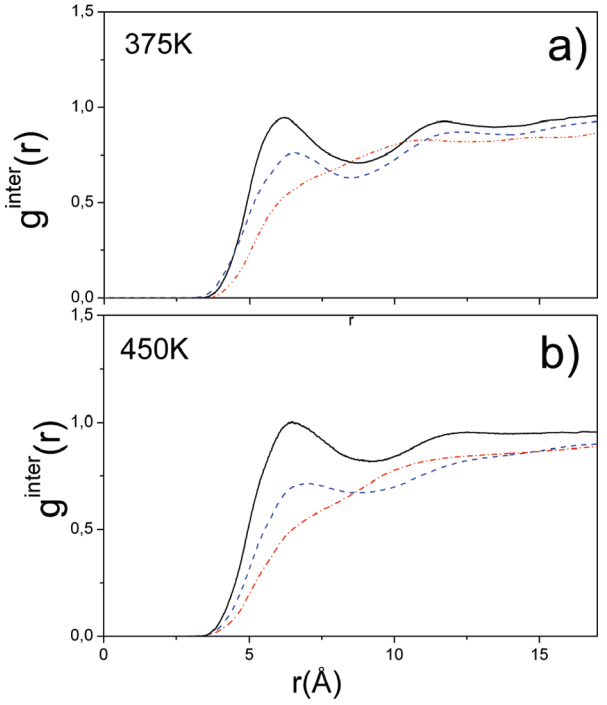

Figure 3. Pair correlation functions: backbone carbons−backbone carbons intermolecular $g(r)$ for PVC (continuous line), PVC15F (dashed line), and PVC50F (dotted-dashed line) at (a) 375 K and (b) 450 K.

density. In order to investigate these questions, the intermolecular pair correlation function $g^{\text{inter}}(r)$ (RDF) between polymer backbone atoms is calculated directly from the simulation. RDF gives an average picture of the local environment of the polymer under consideration, indicating the probability density of finding A and B atoms at a distance of r, averaged over the equilibrium trajectory as

$$g_{a-b}(r) = (V\langle \sum_{i\neq j} \delta(r - |r_{Ai} - r_{Bj}|)\rangle)/(N_A N_B - N_{AB})4\pi r^2 \, dr \quad (1)$$

where i and j refer to the ith and jth atoms of the group A of N_A atoms and B of N_B atoms and N_{AB} is number of atoms common to both groups A and B, angle brackets imply averaging over different configurations. This has been proven to be an effective way of describing the average structure of a polymer material.[33,42,55] Figure 3 shows the rdfs calculated taking into account all polymer backbone carbons: $g^{\text{ie}}{}_{\text{C(bk)-C(bk)}}(r)$ for all the three materials at 375 and 450 K, similar results were obtained at 400 and 425 K (not show here). The subscript "ie" means that only the pairs on different molecules are counted. RDF is conventionally normalized to unit at large separation at which the spatial correlations are lost, and it is zero at short separations when the excluded-volume interaction operates. $g^{\text{ie}}{}_{\text{C(bk)-C(bk)}}(r)$ shows a peak around 5.5 Å for PVC and fluoride−PVC, which can be interpreted as an average interchain distance, followed by one broad shoulder at 10.0 Å. It is worthy to remark that the first peak appears at shorter distances in pure PVC, than in modified PVC. It shifts to larger values as a function of increasing modification degree and temperature. Furthermore, in PVC50F, the lack of a well-developed maximum at ~5.5 Å may be considered as a clear indication of the greater interchain spacing due to the incorporation of 4-fluorothiophenol groups to pristine PVC. The efficiency of packing for these materials can be assessed from the height of the first peak in $g^{\text{ie}}{}_{\text{C(bk)-C(bk)}}(r)$. Pure PVC presents the higher degree of ordering, decreasing the packing efficiency with the degree of modification and temperature. The overall picture is that for highly fluoride PVC, the bulky side groups prevent the backbone atoms to configure themselves maximizing their nonbonded interactions with segments on neighboring chains. It seems that attaching bulky side groups provides a more opened structure that could not only improve the gas diffusivity but also lead to higher gas permeabilities as it has been experimentally observed for other polymers.[7,10,56]

Diffusion Coefficients. From the simulated trajectories, the positions of the gas molecules diffusing in the polymer matrix are computed as a function of time. The diffusion coefficients were calculated from the mean square displacement (MSD) of the penetrant molecules by means of the Einstein−Smoluchowski equation:

$$\langle |r(t) - r(0)|^2 \rangle = 6Dt \quad (2)$$

The brackets show that the average was taken for all the penetrant molecules over all time origins, $r(t)$ is the position vector of the penetrants in space at time t and D is the diffusion coefficient. This equation only applies to the long time limit of the MSD at which the gas molecules have reached the normal diffusive regime characterized by a slope close to unity in the log−log plot of MSD versus time. Representative MSD plots for O_2 and N_2 in PVC and fluoride PVC are shown in Figure 4 at 375 and 450 K. In all the simulated materials the first part of the MSD curve displays a transition from anomalous diffusion,[57] $\langle |r(t) - r(0)|^2 \rangle \cdot \propto \cdot t^n; \cdot n < 1$, to Einstein diffusion ($n = 1$) at about $t < 2$ ns, (with the exception of the ballistic regime at very short times). In the anomalous regime rattling motion within the small cavities dominate the shape of the MSD curve. Jumps between neighboring cavities rarely take place at this time scale. Note that at the highest temperature simulated in this work, the anomalous diffusion regime observed in the MSD curves, finish at shorter simulation times, $t \sim 1$ ns than at 375 K. This would indicate that the transition to a liquid-like diffusion regime has started but it seems that has not totally set up.[33−35] At intermediate temperatures, 400 and 425 K, not shown here, similar plots were obtained displaying a halfway behavior between that observed at the lowest and the highest simulated temperature in this work.

From these plots, it can be clearly appreciated that an increase in the degree of modification of PVC results in an increase of the mobility of the gas molecules. The variation of the mobility of the two gases with the number of 4-fluorothiophenol units incorporated to PVC is very similar. Penetrant mobility is mostly related to two structural features: rigidity of the chains and spacing. Substitution of the chlorine atoms by the bulky 4-fluorothiophenol groups appears to hinder chain packing of the modified PVC. As a consequence, the spacing among polymer chains increase with substitution degree enhancing penetrant mobility. On the other side, as temperature decreases, the local motion of polymer chains is more restricted and differences in penetrant mobility become more evident. These differences are smearing out as temperature increases and the system becomes more isotropic. Local mobility of polymer chains is considered to become an important factor controlling the gas diffusion at temperatures below and close to Tg and it would be discussed later.

Diffusion coefficients of N_2 and O_2 for all the simulated materials are calculated, from the slope of the MSD curves from $t > 100$ ns at 375 K and $t > 50$ ns at $T > 400$ K.

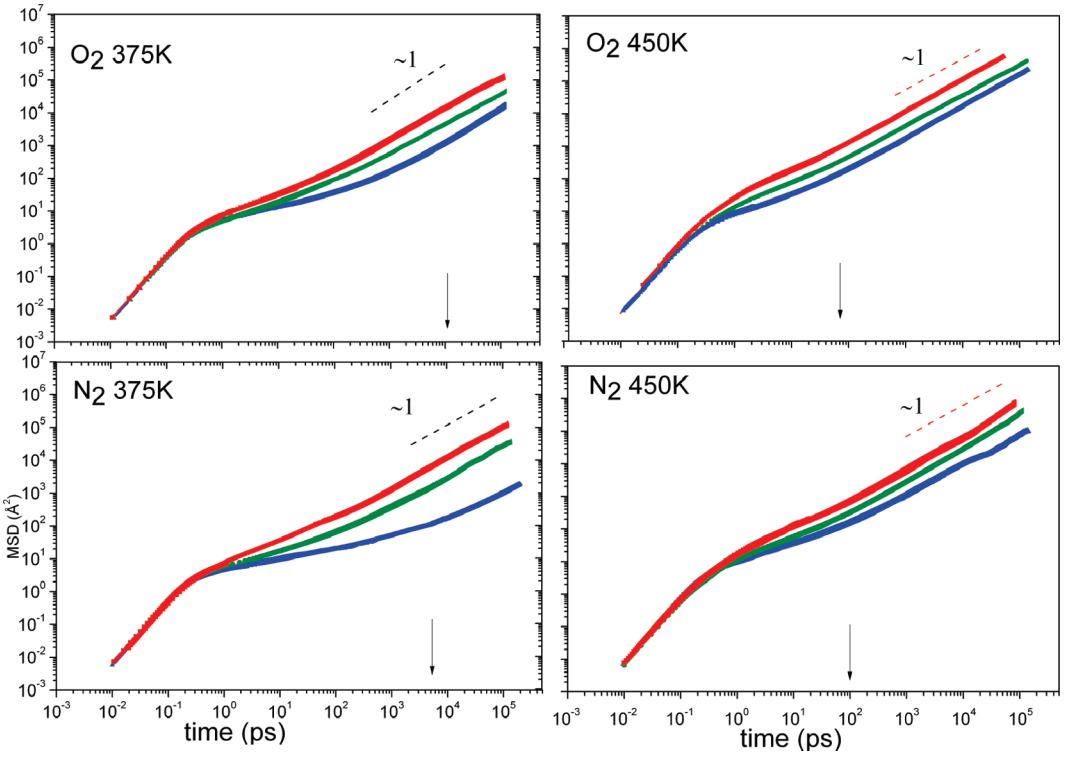

Figure 4. Logarithmic plots: (a) oxygen and (b) nitrogen molecules MSD vs time in PVC (■), lower curve, PVC15F (●), middle curve, and PVC50F (▲) upper curve, at 375 K and 450 K.

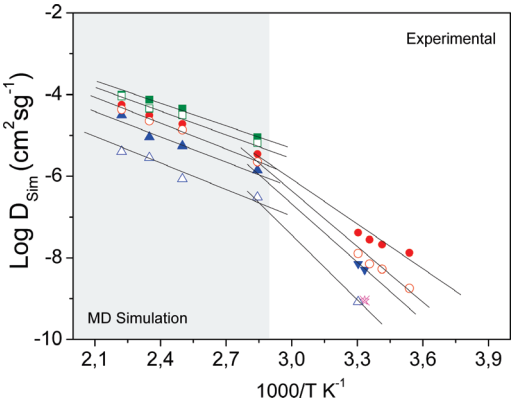

Figure 5. (a) Log of the diffusion coefficient vs reciprocal temperature for O_2 (filled symbols) and N_2 (empty symbols) in PVC (▲), PVC15F, (●) and PVC50F, (■) calculated from MD simulations. Experimental points at $T < 350$ K are from ref 47 and (☼) was calculated for oxygen in PVC using the TST approach.[28]

The natural logarithm of the diffusion coefficient of these gases is plotted against the reciprocal temperature in Figure 5. MD results are presented together with experimental (time-lag) data[49] and calculations using the TST approach[28] at 300 K. The effect of the temperature on the diffusion of O_2 and N_2 can be clearly seen in the increase of the self-diffusion coefficient as well as in the increase of the MSD of the center of mass of the penetrant, Figure 4. In all the cells oxygen has the largest diffusion coefficient, which is mainly due to its smaller volume compared to N_2 and also to its weaker interaction with the polymer matrix. The order of diffusivity is the reverse of the kinetic diameter for each gas. By increasing the molecular size, the diffusivity of the gas decreases. It is worthwhile to point out that upon modification of PVC with 4-fluorothiophenol, there is a 2-fold increase in the diffusion coefficients of both gases through the material. Moreover in this case, this increase in the diffusion coefficient of N_2 and O_2 occurs up to modification degrees of about 50%. However the relative increment with respect to PVC is larger for PVC15F than for PVC50F. This result reflects the influence of the different chain packing efficiency in PVC and PVCF, see Figure 3, on hindering the diffusion of gases through these materials suggesting an important increment in the free volume of the system upon modification. Previous experimental studies on chemically modified PVC with other bulky side groups suggest a similar behavior.[8,10] Furthermore, it is clear that penetrant diffusivities are strongly dependent on temperature. At the lower simulated temperature, 375 K, it is possible to appreciate a slowing down in the penetrant mobility which reveals that the system is approaching to the onset of the polymer transition to the glassy state, where the penetrants spend more of their time trapped in the empty microcavities (accessible free volume).

The activation energy of diffusion, E_d, for O_2 and N_2 in PVC and PVCF can be calculated from this figure by means of the well-known Arrhenius relation, $D = D_o \exp(-E_d/RT)$, where D_o is a constant, E_d is the activation energy, and R is the ideal gas constant. It is apparent that the activation energy is larger in pristine PVC than in fluoride PVC. Below T_g, E_d for O_2 varies between 10.0 and 8.0 kcal mol^{-1}, in pristine PVC and PVCF15, whereas above T_g, E_d goes from 4.5 kcal mol^{-1} for pristine PVC to 3.0 kcal mol^{-1} for PVC50F. The simulations do in fact show that the diffusion is slower in PVC than in PVC15F and PVC50F. The drop in activation energy as temperature increases is clear in all the polymers suggesting a gradual change in the mechanism of diffusion. At low temperature the penetrant is trapped for long periods in a cage surrounded by polymer chains whereas at higher temperature the jumps between neighboring sites become more frequent until the movement is more a liquid-like process. It is convenient to remark that in some polymers

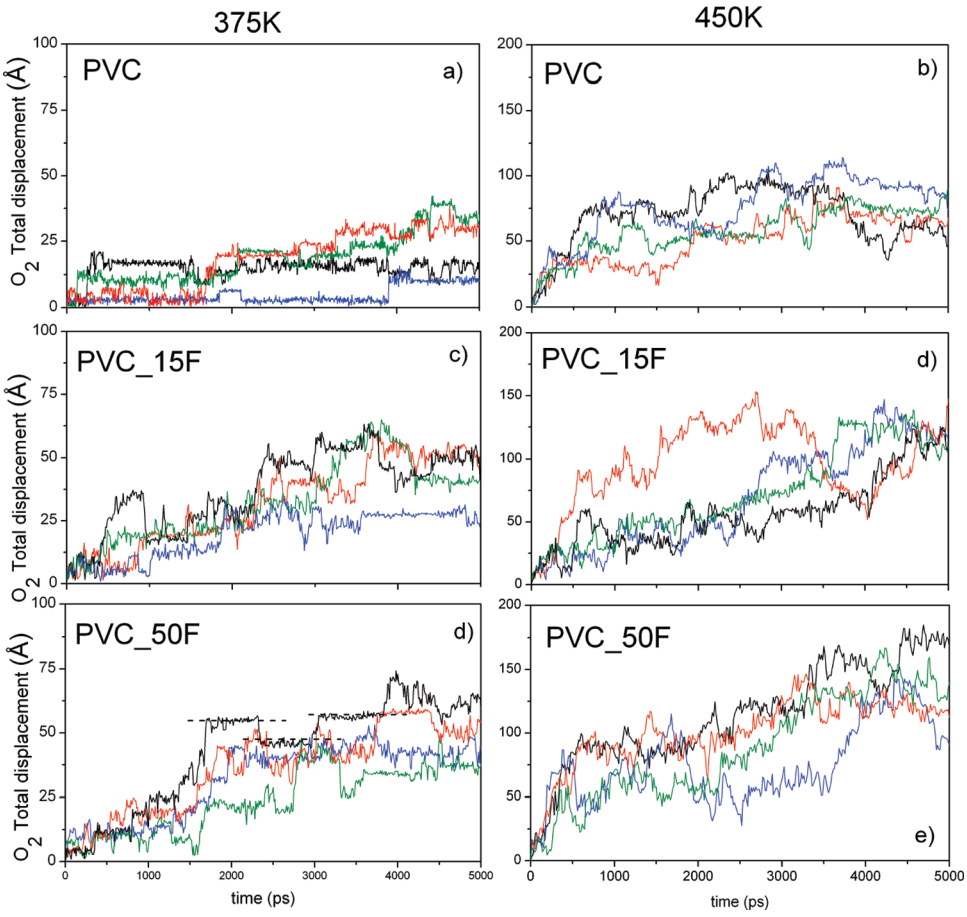

Figure 6. Total displacement of center of mass of oxygen molecules in pristine PVC (a and b), PVC15F (c and d) and PVC50F (e and f) at 375 and 450 K, respectively.

such as, polyisobutylene[58,59] and aromatic polyesters[35] small penetrant diffusion behaves strictly Arrhenius but as it was previously pointed out,[37] this behavior reflects the inability of these polymers to redistribute free volume fast enough in comparison to the difussional motion of the penetrant. In this case, similarly to polyethylene, atactic polypropylene and polybutadiene[34,60] among others, the crossover from a solid-like diffusion mechanism to a liquid-like diffusion mechanism is clearly appreciated. Moreover, the activation energy associated with the diffusion process is higher for N_2 than for O_2 in agreement with the diffusion results. E_d varies between 13.0 and 11.0 kcal mol^{-1} below T_g for pristine PVC and PVC15F, and above T_g, it varies between 6.0 and 4.0 kcal mol^{-1} for PVC nonmodified and PVC50F. From the general accepted picture of the mechanism of the activated diffusion process, it is known that larger cavities need to be formed in the polymer for the diffusion of larger molecules. These will require a larger energy for their formation and hence the activation energy will be larger for the diffusion of larger molecules, and the diffusivity will be smaller.

Analysis of the Diffusion Mechanism. *Mobility of O_2 and N_2 and Free Volume*. One of the objectives of this work is to visualize the diffusion mechanism of small gases in PVC modified with fluoride aromatic thiols. To this end, it is of interest to analyze the trajectories in terms of the type of motions that the penetrants undergo. It is noted that several authors have shown, that for both glassy and rubbery polymers, diffusion proceeds by hoping between different cages.[18,35−37,61,62] For some period of time, the penetrant stays within the cage where it undergoes a rattling motion coupled with an occasional rapid jump to a new cage in a time frame that is short compared with the residence time in the cavity. Thus, the overall diffusion process is a combination of random oscillations of the penetrant molecule inside small cages, interrupted by fast jumps into neighboring cages. This solid-like hopping mechanism can take place at temperatures well above the glass transition temperature due to the short time length of the penetrant's diffusive jumps. However, at higher temperatures a transition from the solid-like diffusion regime into the liquid-like diffusion regime has been observed in several polymers such as, polyisobutylene,[63] polybutadiene[60] and polyethylene[37,64] among others. To illustrate this behavior the motion of the most representative gas molecules inside the polymers at different temperatures has been represented by tracing their displacement from the initial position to their position at time t, $r(t) = (|r(t) - r(0)|^2)^{1/2}$. In Figure 6 we compare oxygen molecules displacement as a function of simulation time in PVC, PVC15F, and PVC50F as quantified by $r(t)$ at 375 and 450 K. Similar plots were obtained for N_2 but are not shown here. In general, the displacement of oxygen molecules through the polymer membranes is larger than for nitrogen which agrees well with previous results. First, it is noted that these figures nicely illustrate the "hopping" mechanism of the penetrant molecules inside a polymer matrix observing several jump events within a simulation time of 5 ns with jump lengths that oscillate between 3 and 10 Å. From these figures, it is clear that the displacement of oxygen and nitrogen molecules is larger in fluoride PVC than in nonmodified-PVC and it appears that its range broadens as the degree of substitution increases. This implies that the oxygen molecules oscillate inside a polymer cavity for a shorter

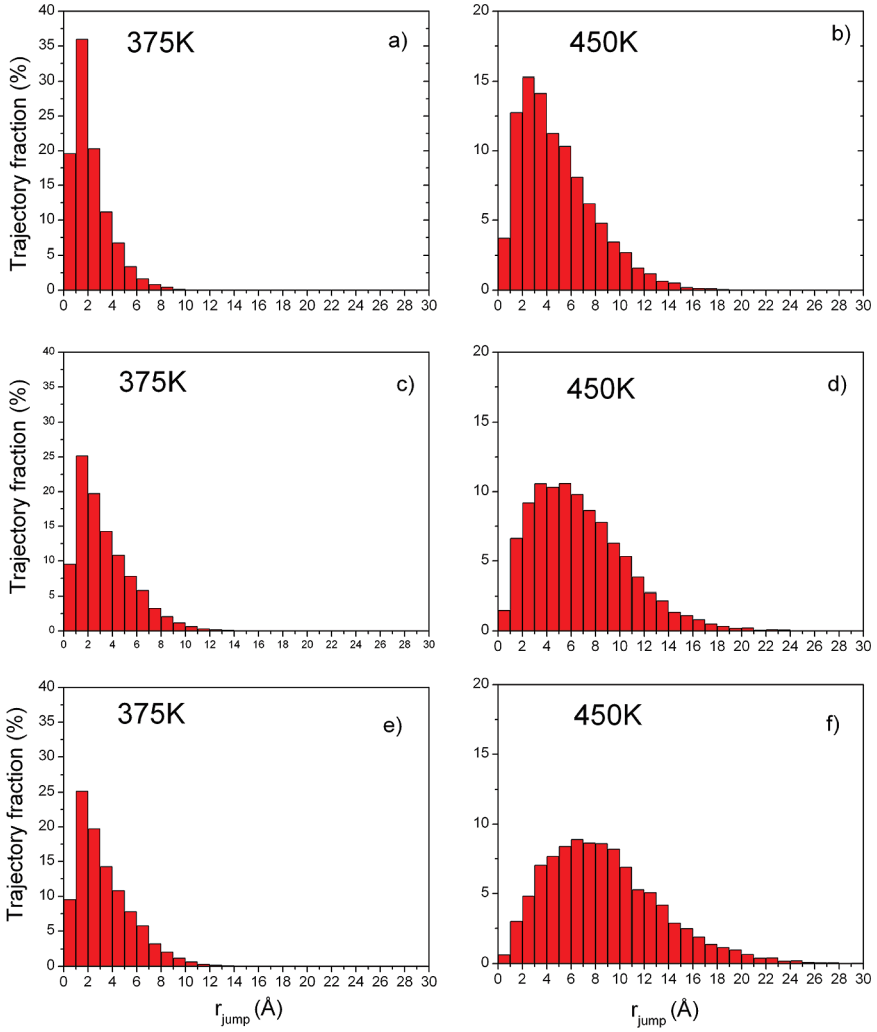

Figure 7. Contribution of jump sizes to the total trajectory for all the O_2 molecules at 375 and 450 K in (a and b) PVC, (c and d) PVC15F and (e and f) PVC50F, respectively.

period of time than N_2 molecules before executing a jump into a neighboring cage. Moreover, from these plots some gas molecules can be identified that jump back and forth between two neighboring holes. This behavior is consistent with the idea of the existence of short lifetime temporary channels between different parts of the free volume with respect to the time spent by the gas molecule inside the cavity, (cage effect).[33,44,65] Turning to the influence of temperature in the diffusion mechanism and comparing data at different temperatures it becomes evident that, at the lowest simulated temperature 375 K, parts a, c and e of Figure 6, the penetrant stays at one place for considerable time and then hops to another place within few picoseconds meanwhile at higher temperatures, the penetrant trajectory is considerably different, parts b, d, and f of Figure 6. The small cavities are still visible but the penetrant spend much less time exploring them because the frequency of jumps increases gradually with the temperature and consequently the quasi-stationary periods between jumps are shorter. It is expected that for even higher temperatures the diffusion process would become continuous. These results confirm the strong temperature dependence of the diffusion coefficients that should similarly manifest in the free volume distribution.

In order to get a further understanding into the diffusion mechanism of gas molecules in fluoride PVC, the diffusive jump distance can be sorted in order of size and placed in size interval bins to get a distribution of jump size contributions to the total trajectory previously analyzed. In this case, to allow a straightforward interpretation of the diffusion process, the penetrant cage motion is removed from the trajectory analysis by a simple filtering process, that is by selecting the appropriate time interval (10−15 ps) to eliminate the cage motion but retain the difussive motion. The distribution of jump lengths of oxygen molecules in PVC and fluoride PVC at 375 and 450 K are shown in Figure 7. It is apparent that jump length distribution significantly broadens as a function of increasing temperature and modification degree of PVC. On the other side, at the lowest temperature, 375 K, the penetrant spend most of its time in localized regions of the polymer, making occasional jumps to neighboring cavities. The distribution is centered in the region of roughly, 2−3 Å, which is approximately the diameter of the penetrant. At this temperature, the motion of the penetrant consists of infrequent jumps separated by long periods of pseudoinactivity. At higher temperature, 450 K, the penetrant trajectories are considerably different and the diffusive regime set at shorter times, see Figure 4. The distribution of jump sizes is largely in the same range but has noticeably broadened with respect to 375 K. Moreover it should be noted that not only the averaged jump length increases with temperature, for PVC from 2 to 5 Å, for PVCF15F from 3 to 8 Å, and for PVC50F from 3 to 9 Å, but also the frequency of diffusive jumps. As a

Table 2. Fractional Free Volume in PVC, PVC15F, and PVC50F As a Function of Temperature

	FFV				
	300 K[a]	375 K	400 K	425 K	450 K
PVC	0.12	0.15	0.18	0.19	0.21
PVC15F	0.14	0.20	0.22	0.24	0.29
PVC50F	0.16	0.21	0.24	0.28	0.37

[a] Fractional free volume calculated from additive group theory.[5]

consequence, the time spent by the penetrant molecules (oscillating motions) inside the cages is shorter, decreasing, both the number of jumps and the jump lengths within the time frame of the simulations in the penetrant order $O_2 > N_2$, i.e., with increasing penetrant size. The values of the estimated and experimental diffusion coefficients decrease in the same order.

The analysis of penetrant trajectories thus suggests a strong dependence of the diffusive process with temperature and modification degree of the pristine PVC. At low temperatures, the penetrant only makes few jumps between long periods of pseudoinactivity in voids in the polymer structure. As the temperature and/or modification degree increases the polymer becomes more mobile and the penetrant is no longer "trapped" in voids, so that the diffusive regime sets in few picoseconds. The jump behavior would suggest that in these polymers at high temperature it is possible to observe a crossover from a solid-like diffusion mechanism to a liquid-like mechanism in good agreement with activation energies calculated above. In addition, these results agree with experimentally and simulated diffusion coefficients[28,49] and can also be interpreted on the basis of the structural modifications introduced in neat PVC. Experimentally it has been found that chemical modification of PVC with bulky side groups simultaneously increases polymer free volume and chain stiffness which obviously facilitates the motion of small gases through the polymer matrix.[8,10] The results for nitrogen in PVC and fluoride PVC, not shown here, are similar to those for oxygen.

It is noted that diffusion of small molecules in polymers depends on several factors such as, temperature, nature of the chemical groups introduced, chain rigidity and free volume among others. The free volume is one of the most significant aspects but equally important is, its distribution and topology.[66−68] Therefore, investigating these aspects can be of paramount importance in analyzing diffusion mechanisms. Fractional free volume, FFV, can be defined as the fraction of the volume not occupied by the polymer and it is directly and accurately determined from simulations. FFV, can be calculated from the well-known empirical equation: $FFV = 1 - V_o/V_s$, where $V_o = 1.3V_w$, V_s is the specific volume, V_o the occupied volume of polymer, and V_w is the van der Walls's volume of polymer that is multiplied by 1.3, based on the packing density of a molecular crystal at 0K. In this study, V_w, was obtained from the volume occupied by van der Waals surface of polymer instead using Bondi's groups. Because V and V_o depend on the temperature of a given sample, it is expected that FFV will likewise vary with temperature. The FFV of PVC, PVC15F, and PVC50F, is calculated according to this expression and listed in Table 2. FFV increases strongly with increasing modification degree of PVC and temperature following the general trends observed experimentally in PVC modified with several reagents.[10] In addition this dependence with temperature and modification degree is consistent with that of the gas diffusion coefficients of O_2 and N_2. However, the calculation of FFV includes some "dead" volume that is no accessible for the gas molecules, whereas the fraction accessible free

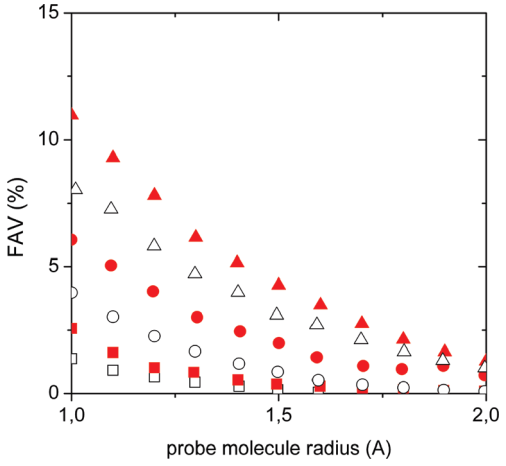

Figure 8. Fractional accessible volume calculated from MD simulations at 375 (empty symbols) and 450 K (filled symbols) of PVC (■), PVC15F (●), and PVC50F (▲), calculated with probes of different radii.

volume, FAV, is defined as the space volume inside a polymer that may be occupied by the center of gravity of penetrant molecules on the condition that the van der Waals spheres of the penetrant do not overlap with the van der Waals spheres of polymer atoms, taking into account only the volume that can be successfully occupied for the gas molecules. FAV seems to be more appropriate for describing the volume available for gas molecules transport,[67] and it has been shown that diffusivity is better correlated to FAV which can be directly determined from MD simulations such as those performed by Hofmann et al.[68] So, in order to investigate the relationship between gas diffusion and polymer structure in PVC and PVCF, FAV was computed by rolling a spherical probe with a given radius to probe the available volume for a particle passing through. Figure 8 illustrates the FAV of PVC, PVC15F and PVC50F at 375 and 450 K calculated by probes with different radii, ranging from 1.0 to 2.0 Å. The probe radii close to the radii of nitrogen and oxygen molecules are found within this range to allow a more direct comparison with gas diffusion experimental results. In the FAV analysis, we found similar results than with the FFV analysis that we mentioned above. It was found that pristine PVC has a lower FAV value than PVC10F and PVC50F. This behavior would indicate that incorporation of aromatic groups to PVC decreased the polymer chain packing efficiency thus forming a larger free volume which is in good agreement with results shown in Figure 3 and with the higher diffusion rates observed for fluoride PVC. On the other hand, we also observed that as temperature increases the FAV increases too, thus providing larger effective free space for gas transport. It suggests that incorporation of bulky side groups to PVC has a larger influence on the accessible free volume than temperature.

As it was mentioned above one of the objectives of this work is to understand how the free volume is distributed in the polymer matrix and its connection to the diffusion mechanism of small gases through it. Figure 9 displays the morphology of the FAV for PVC and PVC50F at 375 and 450 K, and $t = 150$ ns. It is clear from these figures that pristine PVC presents the most compact structure with less empty volume between surrounding polymer chains available for gas transport. The size and shape of this empty volume or cages, and hence the free-volume distribution, change with both temperature and modification degree of PVC. This tendency for a larger FAV value in fluoride PVCs confirms that the bulkiness of the groups incorporated in the

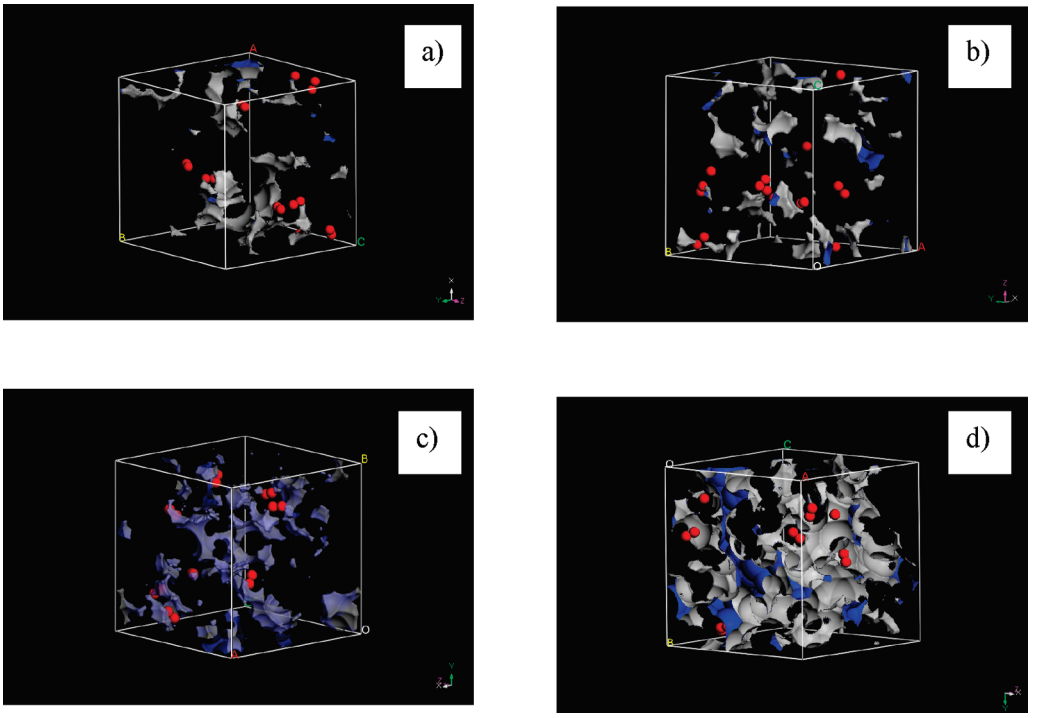

Figure 9. Three-dimensional representation of fractional available free volume in (a and b) PVC and (c−e) PVC50F at 375 and 450 K, respectively, where red spheres represent oxygen molecules.

PVC decrease the polymer chain packing efficiency thus forming larger free volume areas in the polymer matrix. This result is in good agreement with the analysis of the radial distribution functions presented in the previous section. On the other hand, concerning the topology of the FAV, we observed that is strongly dependent on temperature and modification degree of PVC. In this context, it is possible to identify two different scenarios, one for pure PVC where the FAV distribution is formed of many small microvoids and there is not a clear indication of a continuous free volume phase, even at the highest temperature, 450 K and the other for fluoride PVCs where the FAV structure reveals rather large voids with a tendency to form a partly continuous free volume phase. This tendency is more pronounced for the most modified PVC, PVC50F at 450 K. This implies that bulky side groups incorporated in PVC are able to open the structure creating larger regions of free volume. Thus, the amount of free volume created in the samples under study increases with an increase in the 4-fluorothiophenol content and simulation temperature. Obviously, mobility of polymer chain O_2 and N_2 molecules in the system therefore should increase accordingly. This resulted in an increase of the diffusion coefficients of O_2 and N_2 in fluoride PVC with respect to pristine PVC.

Local Dynamics of Polymer Chains. Recently it has been shown how the diffusion of small penetrants in polymers is correlated with the relaxation of polymer chains.[17,69] Therefore, in order to investigate this effect, the local dynamics of the two matrices are compared here through the MSDs of the polymer backbone carbon atoms. Figure 10 shows the averaged MSD curves of the PVC, PVC15F, and PVC50F backbone atoms at 375 and 450 K. The slower motion of backbone atoms together with the enhanced chain packing of pure PVC are one of the main reasons for the slower gas diffusion observed on this polymer compared to modified PVC. Therefore, the higher main chain mobility of fluoride PVC is responsible in part of the large diffusion constants calculated and experimentally determined in these modified

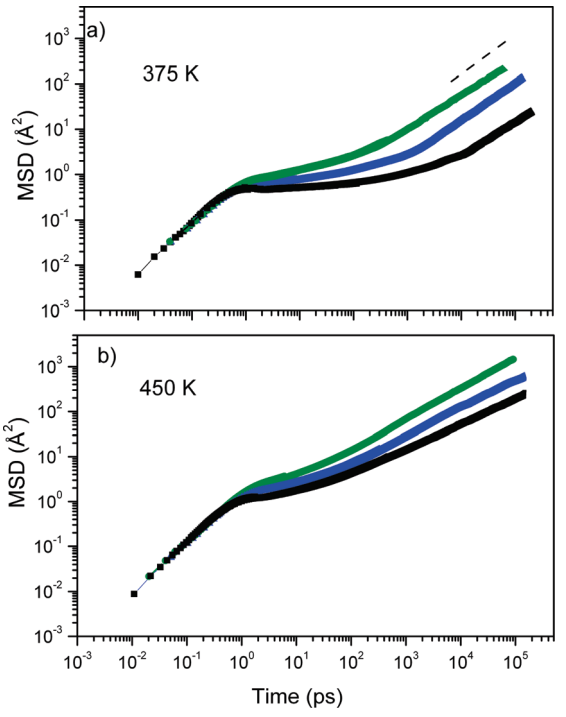

Figure 10. MSD vs time of polymer backbone carbon atoms for PVC (■), PVC15F (▲) and PVC50F (●) at (a) 375 and (b) 450 K.

polymers. In fact, bulky side groups in a polymer usually restrict the local chain mobility and this mainly increases its glass transition temperature. However in this case the 4-fluorothiophenol side group is bonded to the main chain through a sulfur atom which has a double effect, it could enhance rigidity of the polymer chain mainly because of the steric hindrance but it also creates some additional free volume available for diffusion of small gases. An increase in free volume of a polymer is expected to give increased

segmental mobility. The increased segmental mobility will then cause a decrease in the energy required to overcome the interaction between adjacent polymer chains for the gas diffusion process.

On the other hand, in a polymer chain having polar groups and higher CED, see Table 1, the chain mobility is suppressed due to the tighter chain packaging, (e.g., pristine PVC). Comparison of the diffusion coefficients in PVC, PVC15F and PVC50F indicates that CED is more effective in terms of suppressing local mobility than incorporation of bulky side groups.

Conclusions

Molecular dynamic simulations were used to study gas diffusion in PVC modified with 4-fluorothiophenol in the temperature range of 375−450 K. The simulated packing models allow a very detailed determination of structural parameters such as chain packing efficiency, cohesive energy density, fractional free volume, fractional accessible volume and also the distribution of fractional free volume which are not possible through any other technique. Comparison with experimental data at 293 and 298 K for PVC, at 283, 293, 298, and 303 K for PVCF and with results obtained from simulations using the TST approach reveals a very good agreement and highlight the validity of MD simulations in calculating gas transport properties on such materials.

The chain packing structure of modified PVC becomes less structured than that from pure PVC due to the incorporation of bulky side groups. As a consequence of the incorporation of 4-fluorothiophenol to PVC a significant increment in the diffusion coefficients of O_2 and N_2 was observed. The diffusion mechanism is found to change at low temperatures from a pure hopping (solid-like) mechanism to a more liquid-like behavior at higher temperatures as indicated by the change of slope of the Arrhenius plots. In addition, distribution of free volume regions is strongly dependent on both, the number of groups introduced in PVC and temperature. It is observed a transition from few small and dispersed free volume regions in pristine PVC to partly continuous free volume phase in PVCF at the highest temperature simulated in this work. The faster mobility of the backbone atoms in modified PVC compared to pristine PVC together with the lower CED and less efficient chain packing is responsible of the higher diffusion coefficients found in this work. In summary, the replacement of chlorine atoms by 4-fluorothiophenol decreases chain flexibility and also disrupts chain packing efficiency. The bulky side groups increase the free volume and also hinder conformational transitions in PVCF. These two combined effects are responsible of the enhanced gas diffusion properties of fluoride PVC. The results show that the first effect overcomes the second one and strongly influence the gas transport properties in these polymers.

Acknowledgment. The authors acknowledge support from MAT2008-CICYT 1074-48 and J.S. acknowledges support from the CSIC for an I3P tenure track. The authors thank to Galicia Supercomputing Centre, CESGA and CTI, CSIC for generous allocation of CPU time. J.S. thanks Prof. Carsten Menke and M. Entrialgo-Castanõ from Accelrys Inc. for very helpful discussions during the realization of this work.

References and Notes

(1) Kesting, R. E.; Fritzsche, A. K. *Polymeric Gas Separation Membranes*; Wiley-Interscience: New York, 1993.
(2) Paul, D. R.; Yampolskii, Y. P. *Polymeric gas separation membranes*; CRC Press Inc.: New York, 1994.
(3) Sahimi, M. *Flow and Transport in Porous Media and Fractured Rock: From Classical Methods to Modern Approaches*; Wiley-VCH Verlag GmbH: Weinheim, Germany, 1995.
(4) Crank, J.; Park, G. S. Methods of measurement. In *Diffusion in Polymers*; Academic Press: New York, 1968.
(5) Van Krevelen, D. W., *Properties of Polymers: Their Correlation with Chemical Structure; Their Numerical Estimation and Prediction from Additive Group Contributions*; Elsevier: Netherlands, 1990.
(6) Tiemblo, P.; Mártinez, G.; Gómez-Elvira, J. M.; Millán, J. *Polym. Bull.* **1994**, *32*, 353–359.
(7) Tiemblo, P.; Fernandez-Arizpe, A.; Riande, E.; Guzman, J. *Polymer* **2003**, *44*, 635–641.
(8) Tiemblo, P.; Guzman, J.; Riande, E.; Mijangos, C.; Reinecke, H. *Macromolecules* **2001**, *35*, 420–424.
(9) Poulsen, L.; Zebger, I.; Klinger, M.; Eldrup, M.; Sommer-Larsen, P.; Ogilby, P. R. *Macromolecules* **2003**, *36*, 7189–7198.
(10) Tiemblo, P.; Guzmán, J.; Riande, E.; Mijangos, C.; Herrero, M.; Espeso, J.; Reinecke, H. *J. Polym. Sci., Part B: Polym. Phys.* **2002**, *40*, 964–971.
(11) Lin, H.; Freeman, B. D. *Macromolecules* **2006**, *39*, 3568–3580.
(12) Khalikov, R. M.; Kozlov, G. V.; Zaikov, G. E. *J. Appl. Polym. Sci.* **2006**, *99*, 3571–3573.
(13) Tiemblo, P.; Guzmán, J.; Riande, E.; Salvador, E. F.; Peinado, C. *J. Polym. Sci., Part B: Polym. Phys.* **2001**, *39*, 786–795.
(14) Theodorou, D. N. *Diffusion in polymers*; Marcel Dekker Inc.: New York, 1996.
(15) Muller-Plathe, F. *J. Chem. Phys.* **1995**, *103*, 4346–4351.
(16) Cuthbert, T. R.; Wagner, N. J.; Paulaitis, M. E. *Macromolecules* **1997**, *30*, 3058.
(17) Kucukpinar, E.; Doruker, P. *Polymer* **2006**, *47*, 7835–7845.
(18) Muller-Plathe, F. *J. Chem. Phys.* **1991**, *94*, 3192–3199.
(19) Chang, M. L.; Xiao, Y.; Chung, T. S.; Toriida, M.; Tamai, S. *Polymer* **2007**, *48*, 311–317.
(20) Hofmann, D.; Fritz, L.; Ulbrich, J.; Schepers, C.; Böhning, M. *Macromol. Theory Simul.* **2000**, *9*, 293–327.
(21) Muller-Plathe, F. *J. Chem. Phys.* **1992**, *96*, 3200–3205.
(22) Tsolou, G.; Mavrantzas, V. G.; Makrodimitri, Z. A.; Economou, I. G.; Gani, R. *Macromolecules* **2008**, *41*, 6228–6238.
(23) Boyd, R. H.; Pant, P. V. K. *Macromolecules* **2002**, *24*, 6325–6331.
(24) Ennari, J.; Pietilä, L.-O.; Virkkunen, V.; Sundholm, F. *Polymer* **2002**, *43*, 5427–5438.
(25) Pavel, D.; Shanks, R. *Polymer* **2003**, *44*, 6713–6724.
(26) Zhang, Q. G.; Liu, Q. L.; Wu, J. Y.; Chen, Y.; Zhu, A. M. *J. Membr. Sci.* **2009**, *342* (1−2), 105–112.
(27) Gusev, A. A.; Arizzi, S.; Suter, U. W.; Moll, D. J. *J. Chem. Phys.* **1993**, *99*, 2221–2227.
(28) Tiemblo, P.; Saiz, E.; Guzman, J.; Riande, E. *Macromolecules* **2002**, *35*, 4167–4174.
(29) Gusev, A. A.; Suter, U. W. *J. Chem. Phys.* **1993**, *99*, 2228–2234.
(30) Heuchel, M.; Fritsch, D.; Budd, P. M.; McKeown, N. B.; Hofmann, D. *J. Membr. Sci.* **2008**, *318* (1−2), 84–99.
(31) Heuchel, M.; Hofmann, D.; Pullumbi, P. *Macromolecules* **2004**, *37*, 201–214.
(32) Neyertz, S. *Macromol. Theory Simul.* **2007**, *16*, 513–524.
(33) Han, J.; Boyd, R. H. *Polymer* **1996**, *37*, 1797–1804.
(34) Meunier, M. *J. Chem. Phys.* **2005**, *123*, 134906–7.
(35) Bharadwaj, R. K.; Boyd, R. H. *Polymer* **1999**, *40*, 4229–4236.
(36) Milano, G.; Guerra, G.; Muller-Plathe, F. *Chem. Mater.* **2002**, *14*, 2977–2982.
(37) van der Vegt, N. F. A. *Macromolecules* **2000**, *33*, 3153–3160.
(38) Boshoff, J. H. D.; Lobo, R. F.; Wagner, N. J. *Macromolecules* **2001**, *34*, 6107–6116.
(39) *Materials Studio 4.4, V. amorphous cell, discover and forcite+ modules*; Accelrys Inc.: San Diego, CA, 2005.
(40) Sun, H. *J. Phys. Chem.* **1998**, *B102*, 7338–7364.
(41) Rigby, D.; Roe, R.-J. *J. Chem. Phys.* **1987**, *87*, 7285–7290.
(42) Sacristan, J.; Mijangos, C. *J. Chem. Phys.* **2008**, *129*, 20.
(43) Rigby, D.; Sun, H.; Eichinger, B. E. *Polym. Int.* **1997**, *44*, 311–330.
(44) Tocci, E.; Bellacchio, E.; Russo, N.; Drioli, E. *J. Membr. Sci.* **2002**, *206* (1−2), 389–398.
(45) Ewald, P. P. *Ann. Phys.* **1921**, *64*, 253.
(46) Berendsen, H. J. C.; Postma, J. P. M.; Gunsteren, W. F. v.; DiNola, A.; Haak, J. R. *J. Chem. Phys.* **1984**, *81*, 3684–3690.
(47) *Synthia*; Accelrys Inc.: San Diego, CA, 2010.
(48) Bicerano, J. *Prediction of Polymer Properties*; Marcel Dekker Inc.: New York, 2002.
(49) Brierbauer, K.; Lopez, M.; Mijangos, C.; Riande, E. *J. Membr. Sci.* **2010**, doi:10.1016/j.memsci.2010.06.035.
(50) Makrodimitri, Z. A.; Economou, I. G. *Macromolecules* **2008**, *41*, 5899–5907.
(51) Gestoso, P.; Meunier, M. *Mol. Simul.* **2008**, *34*, 1135–1141.

(52) Kusuma, V. A.; Freeman, B. D.; Jose-Yacaman, M.; Lin, H.; Kalakkunnath, S.; Kalika, D. S. Structure/Property Characteristics of Polar Rubbery Membranes for Carbon Dioxide Removal. In *Advanced Membrane Technology and Applications*; Norman, N. L., Fane, A. G., Winston Ho, W. S., Matsuura, T.; Eds.; John Wiley & Sons., Inc.: Hoboken, New Jersey, **2008**; pp 929−953.
(53) Koros, W. J.; Coleman, M. R.; Walker, D. R. B. *Annu. Rev. Mater. Sci.* **1992**, *22* (1), 47–89.
(54) Fedors, R. F. *Polym. Eng. Sci.* **1974**, *14*, 147.
(55) Neelakantan, A.; Stine, R.; Maranas, J. K. *Macromolecules* **2003**, *36*, 3721–3731.
(56) Ayala, D.; Lozano, A. E.; de Abajo, J.; García-Perez, C.; de la Campa, J. G.; Peinemann, K. V.; Freeman, B. D.; Prabhakar, R. *J. Membr. Sci.* **2003**, *215*, 61–73.
(57) Gusev, A. A.; Müller-Plathe, F.; van Gunsteren, W. F.; W., S. U., *Atomistic Modeling of Physical Properties*; Springer: Berlin and Heidelberg, Germany, 1994; Vol. *116*.
(58) Han, J.; Boyd, R. H. *Macromolecules* **1994**, *27*, 5365–5370.
(59) Han, J.; Boyd, R. H. *Polymer* **1996**, *37*, 1797–1804.
(60) Gee, R. H.; Boyd, R. H. *Polymer* **1995**, *36*, 1435–1440.
(61) Sok, R. M.; Berendsen, H. J. C. *J. Chem. Phys.* **1992**, *96*, 4699.
(62) Takeuchi, H.; Okazaki, K. *J. Chem. Phys.* **1990**, *92*, 5643.
(63) Pant, P. V. K.; Boyd, R. H. *Macromolecules* **2002**, *26*, 679–686.
(64) Gee, R. H.; Boyd, R. H. *Comput. Theor. Polym. Sci.* **1998**, *8* (1−2), 93–98.
(65) Hofmann, D.; Fritz, L.; Ulbrich, J.; Paul, D. *Polymer* **1997**, *38*, 6145–6155.
(66) Heuchel, M.; Böhning, M.; Hölck, O.; Siegert, M. R.; Hofmann, D. *Desalination* **2006**, *199* (1−3), 443–444.
(67) Chang, K.-S.; Tung, C.-C.; Wang, K.-S.; Tung, K.-L. *J. Phys. Chem. B* **2009**, *113*, 9821–9830.
(68) Hofmann, D.; Entrialgo-Castano, M.; Lerbret, A.; Heuchel, M.; Yampolskii, Y. *Macromolecules* **2003**, *36*, 8528–8538.
(69) Pant, P. V. K.; Boyd, R. H. *Macromolecules* **1993**, *26*, 679–686.